PAPER www.rsc.org/PCCP| Physical Chemistry Chemical Physics

Resolution and Polarization Distribution in Cryogenic DNP/MAS Experiments

Alexander B. Barnes,[a] Björn Corzilius,[a] Melody L. Mak-Jurkauskas,[a,b] Loren B. Andreas,[a] Vikram S. Bajaj,[a] Yoh Matsuki,[b] Marina Belenky,[b] Johan Lugtenburg,[d] Jagadishwar R. Sirigi,[c] Richard J. Temkin,[c] Judith Herzfeld,[b] and Robert G. Griffin*[a]

Received (in XXX, XXX) Xth XXXXXXXXX 2010, Accepted Xth XXXXXXXXX 2010
First published on the web Xth XXXXXXXXX 2010
DOI: 10.1039/b000000x

This contribution addresses four common misconceptions associated with high-resolution dynamic nuclear polarization/magic angle spinning (DNP/MAS) experiments. First, spectral resolution is not generally compromised at the cryogenic temperatures at which DNP experiments are performed. As we demonstrate at a modest field of 9 Tesla (380 MHz ^{1}H), 1 ppm linewidths are observed in DNP/MAS spectra of membrane protein in its native lipid bilayer, and <0.4 ppm linewidths are reported in a crystalline peptide at 85 K. Second, we address the concerns about paramagnetic broadening in DNP/MAS spectra of proteins by demonstrating that the exogenous radical polarizing agents utilized for DNP are distributed in the sample in such a manner as to avoid paramagnetic broadening and thus maintain full spectral resolution. Third, the enhanced polarization is not localized around the polarizing agent, but rather is effectively and uniformly dispersed throughout the sample, even in the case of membrane proteins. Fourth, the distribution of polarization from the electron spins mediated via spin diffusion between ^{1}H-^{1}H strongly dipolar coupled spins is so rapid that shorter magnetization recovery periods between signal averaging transients can be utilized in DNP/MAS experiments than in typical experiments performed at ambient temperature.

Introduction

Dynamic nuclear polarization (DNP) increases polarization in the bulk nuclear spin bath by 2-3 orders of magnitude,[1-3] and thus results in a significant gain in the sensitivity of NMR experiments. Concurrently, the excellent resolution available with contemporary magic angle spinning (MAS) instrumentation and methods is not compromised by DNP, establishing DNP/MAS as a sensitive and high-resolution spectroscopic technique of great utility for structural characterization of membrane proteins in lipid layers[4, 5], amyloid fibrils[6], and crystalline peptides and proteins.[7]

Generally, unpaired electrons in stable, soluble, exogenously introduced free radicals are the source of the high Boltzman polarization for DNP experiments.[8] In particular, biradicals are used as polarizing agents at high field, because they can take full advantage of the cross effect (CE), an electron-nuclear polarization transfer mechanism that performs well at high frequencies.[9] These polarizing agents can be used at sufficiently low concentration to be statistically separated from the spins of interest, and are therefore not in direct dipolar contact with the bulk nuclei detected in MAS NMR experiments. Nevertheless, they still perform as effective sources of polarization. On the other hand, high concentrations of radicals can be used when they are sterically excluded from the sites of interest.[7] In either case, the absense of direct electron-nuclear dipolar couplings between the unpaired electron spins and the detected nuclear spins has important implications.

First, an efficient transfer scheme is required to distribute the high polarization from the shell of directly electron-coupled nuclear spins to the bulk of the sample. In the case of protonated biological samples, the ~100 M concentration of ^{1}H spins, with their high gyromagetic ratio, provide a sufficiently strongly coupled spin bath to uniformly distribute polarization throughout the medium, even if the sample is a heterogenous mixture comprised of cryoprotectant and membrane protein embedded in native lipid bilayers.[10] Proton spin diffusion distributes the polarization originating from the electrons to the entirety of the sample within hundreds of milliseconds, thereby permiting short magnetization recovery delays between signal averaging transients.

Also, because the ^{1}H spin diffusion and subsequent cross polarization (CP) polarize nuclei that are well separated from

[a]*Department of Chemistry and Francis Bitter Magnet Laboratory, Massachusetts Institute of Technology, Cambridge, MA 02139, USA*
[b]*Department of Chemistry, Brandeis University, Waltham, MA 02454, USA*
[c] *Plasma Science and Fusion Center, Massachusetts Institute of Technology, Cambridge, MA 02139, USA*
[d] *Department of Chemistry, University of Leiden, The Netherlands*
**Corresponding author. Fax: +1 617 253 5405.*
E-mail address: rgg@mit.edu (R.G. Griffin).
†

the biradicals, spectral resolution is not compromised by the presence of the paramagnetic polarizing agents. Due to the relatively low gyromagnetic ratio of the ^{15}N and ^{13}C, the nuclei most commonly detected in biomolecular MAS experiments, the paramagnetic electron spin must be relatively close (~10 Å) to induce pseudo-contact shifts and line broadening. In fact, Nadaud and colleagues recently showed that even when a nitroxide label is covalently bound to a small globular protein, only spins in relatively close proximity are affected by the spin label.[11] In the case of most DNP experiments, the biradicals are simply present in the matrix, not covalently bound to the protein of interest, and thus not in close spatially proximity to the detected spins.

However, even with very efficient spin-diffusion, the temperature must still be lowered to ≤100 K to lengthen the e^- and ^1H T_1 relaxation times sufficiently for relayed transfer of enhanced magnetization throughout the sample. The resolution of MAS spectra at these temperatures is a point of concern in the solid state NMR community. However, although the resolution of some spectra degrade at low temperatures, either due to improper cryoprotection or trapped conformational heterogeneity, we demonstrate here that high-resolution spectra of a membrane protein and crystalline peptides can be acquired at temperatures below 100 K. We also show spectra for a peptide in which some of the resonances heterogenously broaden at lower temperature, while other resonances remain narrow.

Experimental

Membrane Preparation

[14-^{13}C]retinal,[ε-^{13}C]lysine-labeled bacteriorhodopsin (bR) was obtained as indicated by Griffiths *et al.*[12] [ζ-^{15}N]lysine-labeled bR was obtained as described by Argade *et al.*[15] Uniformly ^{13}C,^{15}N-labeled bR was obtained as set out by Bajaj *et al.*^PNAS 2009, **106**: 9244-9249^ The purple membranes were isolated according to the method of Oesterhelt and Stoeckenius[14], washed in 0.3 M guanidinium hydrochloride at pH 10, until the supernatant had the same pH, and then washed further with 60 vol% d_8-glycerol, 40 vol% aqueous 0.3 M Guanadine·HCl (pH = 10), which acts as a cryoprotectant. The concentration of the nonperturbing biradical polarizing agent, TOTAPOL[13] was 15-20 mM. Membranes were collected in a pellet by ultracentrifugation (5 h at 323,000 *g*) and packed into a 4-mm OD, single-crystal sapphire rotor that is transparent at both optical and microwave wavelengths.

Peptide Preparation

N-*formyl*-Met-Leu-Phe-OH (N-*f*-MLF-OH) was obtained from Bachem (King of Prussia, PA). Uniformly ^{13}C,^{15}N-labelled N-*f*-MLF-OH was synthesized by CS Bio Inc. (Menlo Park, CA) and diluted with natural abundance compound. In each case, the peptide was recrystallized from isopropanol. Small, needlelike crystals were obtained after dissolution in warm solvent and subsequent drying.

Uniformly ^{13}C,^{15}N-labeled Alanyl-prolyl-glycine (APG) was also diluted to 10% with the corresponding natural abundance tripeptide. The tripeptide was synthesized by CS Bio (Menlo Park, CA) with labeled amino acids from Cambridge Isotopes (Andover, MA) and BaChem (Switzerland). APG was recrystallized from water. The peptide, dissolved in a minimal amount of water (the solubility was approximately 45 mg/ml), produced crystals within a week of being placed in a desiccator next to a container of excess ethylene glycol.

All peptide crystals were crushed and packed in 4 mm zirconia rotors. The drive-tips on all of the rotors ware bonded to the rotor sleeve with a low-temperature epoxy as described by Barnes et al.[16]

Instrumentation

All spectra were collected on a custom-built 250 GHz, 380 MHz, 95 MHz, 38 MHz (e^-,^1H,^{13}C,^{15}N) frequency spectrometer (courtesy of D. J. Ruben). The quadruple resonance MAS probe is equipped with a cryogenic sample exchange system, microwave transmission circuit, and a fiber-optic for *in situ* optical illumination of the sample, as described by Barnes *et al.*[16] Details of the 250 GHz gyrotron, corrugated microwave transmission line, and heat exchanger can be found elsewhere.[17-20]

Accumulation of bR photointermediates

Accumulation of bR photointermediates was performed *in situ*, via optical irradiation from a fiber-optic while the rotor was spinning in the MAS module. In this manner, access to the full temperature range of the probe can be utilized to both the accumulate photointermediates at the appropriate temperature and cryogenically trap them at ~90 K for data acquisition in the dark. At such low temperatures the lifetimes of the photointermediates can be extended indefinitely. For example, experiments were performed on the M_o intermediate for over a month without the protein relaxing to intermediates further along the photocycle.

bR_{568} was accumulated by irradiating dark-adapted bR (a thermally equilibrated mixture of bR_{555} and bR_{568}) at 273 K with 1 W of 532 nm irradiation for 90 minutes. The M_o photocycleintermediate was accumulated by irradiating light adapted bR at 210 Kwith 1 W of 532 nm light for 120 minutes.

Results and Discussion

High resolution spectra of the active site of a membrane protein

Fig. 1 shows well-resolved correlation spectra of bR embedded in its native lipid bilayer. We emphasize that we acquired these spectra with samples containing 15-20 mM TOTAPOL (i.e., 30-40 mM electrons) and that they do not show signs of paramagnetic broadening. The high signal-to-noise ratio available with the boost in nuclear polarization from DNP enable otherwise inaccessible quantitative measurements.[16] Here we discuss the narrow linewidths and excellent site-resolution seen in the spectra. We emphasize two strategies, selective labelling and editing on the basis of unique chemical shifts, to acquire well-resolved spectra of this

large (26 kD) membrane protein at a modest field of 9 Tesla, as shown in Fig. 1.

Fig. 1a and Fig. 1b show resolved ^{13}C-^{13}C correlation spectra of [14-^{13}C]retinal covalently bound to [ε–^{13}C]lysine in bR.[12] Strategically labelling sites of interest is a well-established technique to reduce spectral crowding and acquire high-quality distance constraints, although we also note that this strategy reduces the amount of structural information that can be extracted from a given sample. Nonetheless, crosspeaks arising from the two states present in the dark-adapted protein are clearly resolved and exhibit narrow resonances. The slightly larger linewidth of the bR_{555} resonances is a manifestation of the previously characterized heterogeneity of bR_{555}.[18] The bR_{568} cross peak has a linewidth of 1.2 ppm in the C14 direct dimension (Fig. 1a) and 1 ppm (95 Hz) in the Cε direct dimension (Fig. 1b). These are the narrowest resonances of a membrane protein from DNP/MAS experiments reported thus far in the literature. However, we expect optimization of the lipid environment and cryoprotectant as well as extension of DNP to higher magnetic fields to lead to still higher resolution.

The spectrum in Fig. 1c utilizes the single site resolution available in the spectrum of uniformly ^{13}C,^{15}N-labelled bR. The Schiff base situated in the active site of the protein has a unique chemical environment that manifests as a ^{15}N chemical shift well-resolved from the other nitrogen resonances. Therefore, experiments that first evolve an indirect ^{15}N chemical shift evolution will yield single site resolution from the Schiff base and result in resolved, high-quality spectra. Reducing the spectral crowding in the ^{13}C dimension by limiting the observed resonances to spins in close proximity to the single resolved nitrogen resonance yields excellent resolution and the capability to simultaneously assign multiple carbon resonances in the active site of the protein. This strategy of tranferring polarization from a site which is resolved in the indirect dimension, either by existing in a unique chemical environment, like the Schiff base in bR, or by selective isotopic labelling, yields resolved spectra of high molecular weight systems even at relatively low magnetic fields (9 T).

High resolution MAS spectra of peptides from 75 to 273 Kelvin

The dearth of instrumentation capable of acquiring high-

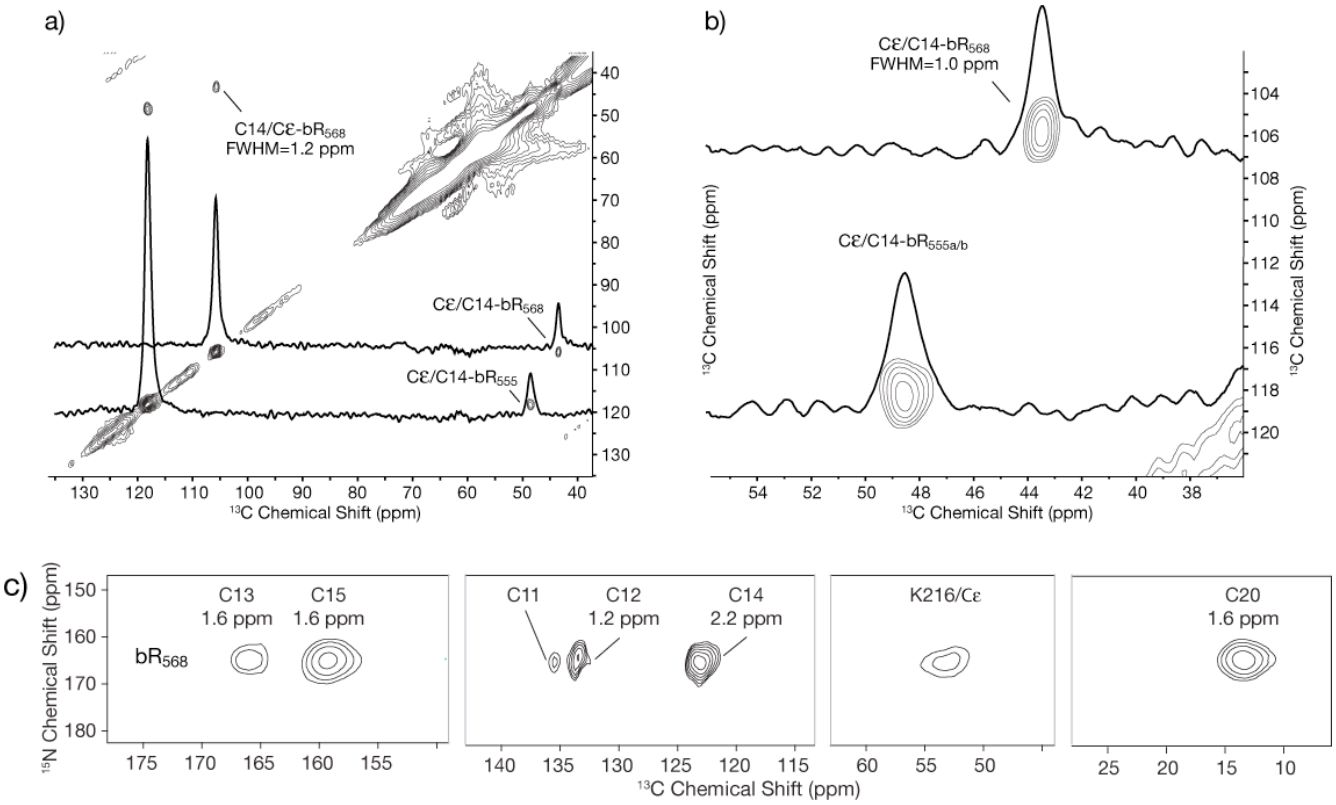

Fig. 1 High resolution DNP spectra of bR. a) RFDR correlation spectrum of 14 mg of [14-^{13}C]retinal, [ε–^{13}C]lysine-labeled bR in the dark-adapted state with 1D direct ^{13}C dimension slices overlaid on the 2D contours. 12.5 days worth of acquisition time from mixing times between 8 and 28 ms were averaged together. The resulting signal-to-noise negated the need for any line-broadening. The bR_{568} correlation in the upper left has a linewidth of 1.2 ppm (115 Hz) b) Expansion of the lower right portion of the spectrum in (a) demonstrating the narrow linewidths achievable with MAS DNP. Whereas the bR_{555} correlation is slightly broader due to the presence of two conformations of bR_{555}, the bR_{568} resonance is extremely narrow with a linewidth of 1.0 ppm (95 Hz). c) Carbon-nitrogen 2D spectrum of uniformly ^{13}C,^{15}N-labeled bR_{568}.[21] After an indirect chemical shift evolution on the resolved Schiff base (165 ppm in the ^{15}N dimension), the magnetization is transferred along the retinal chain all the way to C11, and also in the other direction directly to Cε. The carbon resonances show relatively narrow linewidths (1.2-2.2 ppm).

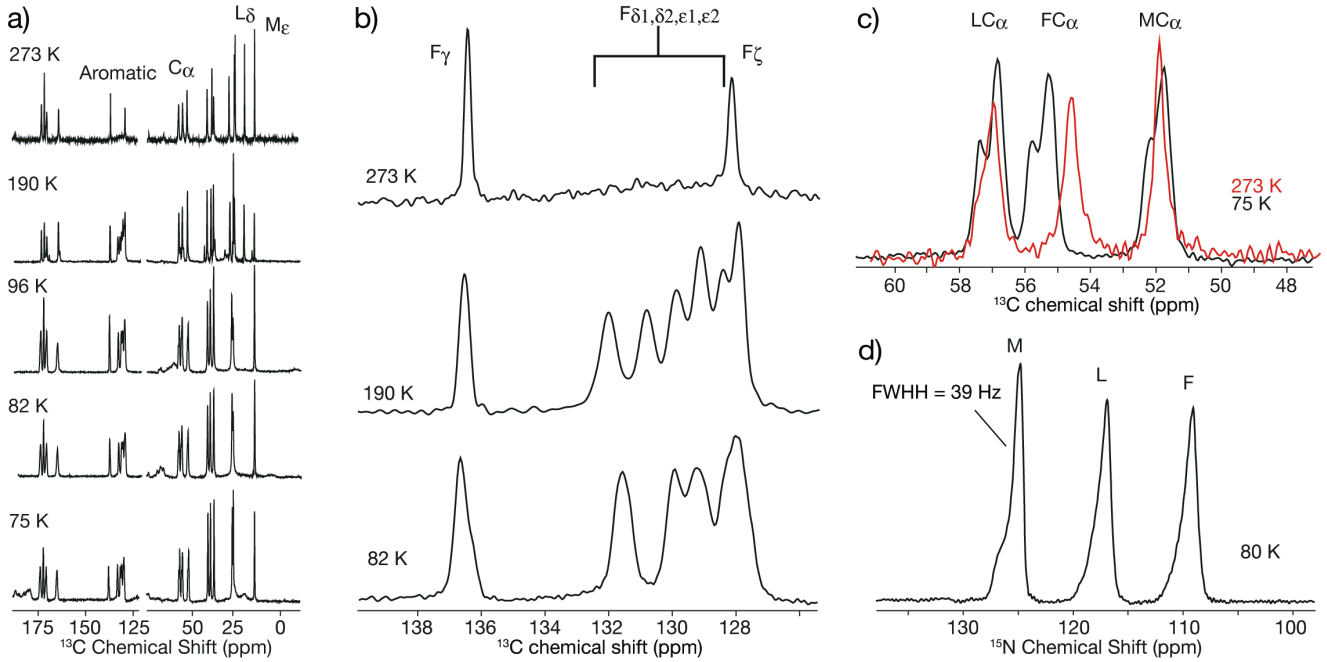

Fig. 2 Temperature dependent, high-resolution cryogenic MAS spectra of N-*f*-MLF-OH. a) ^{13}C spectra from 273 K to 75 K showing that excellent resolution is maintained throughout the 200 K temperature range. b) Expansion of the aromatic regions at 273, 190, and 82 K showing resolved resonances, even with coexisting conformations at 190 K. c) Expansion of the alpha carbon region showing the resolved resonances of the two conformations present at 75 K, each different from the resonances of the single conformation observed at 273 K. d) ^{15}N spectrum of [U-^{13}C,^{15}N]-N-*f*-MLF-OH. The shoulder on each resonances is a manifestation of the two conformations present at 75 K. Nonetheless excellent resolution (linewidths of 39 Hz) is still maintained at 75 K.

resolution spectra at cryogenic temperatures has contributed to the misconception that MAS spectra are always broader at cryogenic temperatures. High resolution at 90K (0.3 ppm, 30 Hz) has recently been demonstrated in conjunction with the development of a cryogenic sample exchange DNP probe.[16] Here, we elaborate further on the high resolution available in MAS spectra between 75K and 273K. We focus on crystalline tripeptides, because they do not contain bulk water that necessitates the use of a cryoprotectant, such as glycerol, to maintain long-range homogeneity at low temperatures.

(i) N-*formyl*-Met-Leu-Phe-OH (N-*f*-MLF-OH)

Fig. 2 shows high-resolution ^{13}C MAS spectra of crystalline natural abundance N-*f*-MLF-OH recorded from 273 to 75 K and ^{15}N spectra of uniformly ^{13}C,^{15}N-labelled peptide at 80 K. All of the resonances are narrow (<0.6 ppm, 60 Hz) over the entire temperature range. An expansion of the aromatic region is shown in Fig. 2b. The top spectrum at 273 K shows only the Fζ resonance because the 2-fold flipping of the phenylalanine ring interferes with the ^{1}H decoupling field, broadening the δ,δ' and ε,ε' aromatic resonances beyond the detection limit.[22] However, the dynamics slow down at 190 K revealing resonances arising from two coexisting forms of the peptide. Without proper optimization of the homogeneiety and the magic angle, this spectral crowding leads to an apparent broadening. However, the spectrum in Fig. 2b at 190 K clearly shows that nearly all of the single aromatic resonances are resolved from one another. Each single resonance is not by itself appreciably broader than resonances at room temperature.

An expansion of the C_α region is shown in Fig. 1c revealing two backbone conformations present at 75 K. The two coexistent forms are manifest as a doubling of the resonances, while each of the lines comprising the doublet remains narrow. We attribute this to a small change in torsion angles rather than a globally different structure because the Mε resonance is still extremely sharp <30 Hz at 75 K, indicating a lack of heterogeneous broadening due to freezing the peptide. The two low temperature conformations are also apparent in the asymmetric lineshapes of the ^{15}N resonances (Fig. 1d). In a similar ratio to that seen in the Cα region of the ^{13}C spectrum, the two conformations are manifest as a single ^{15}N resonance with a shoulder; the dominant resonances however remains narrow (only 39 Hz for the amide of Met). We emphasize that the ^{15}N spectrum was acquired on a uniformly ^{13}C,^{15}N-labelled sample, thus the ^{15}N-^{13}C J-coupling contributes to the linewidths in the spectrum.

(ii) Alanyl-proyl-glycine (APG)

To demonstrate that the resolution seen in the N-*f*-MLF-OH spectra are not unique to a single system, we also show comparable resolution in cryogenic MAS spectra of another tripeptide, APG. APG is different from N-*f*-MLF-OH in two important aspects. First, the crystal lattice contains one water molecule per unit cell that we show does not lead to significant broadening of resonances at low temperatures. Secondly, the proline ring samples two puckered conformations, a structural feature of five-membered rings that has been well characterized in the literature[23, 24] and has also been observed in both the X-ray and solid state NMR structures of APG.[25] We emphasize that in contrast to the ^{13}C spectra of natural abundance N-*f*-MLF-OH in Fig. 2, the ^{13}C spectra in Fig. 3 are taken of uniformly ^{13}C,^{15}N-labelled APG.

Examination of the linewidths at 293 K and 75 K in Fig. 3a reveals that most of the ^{13}C lines remain narrow (broadening <17 Hz) at 75 K, including the Pα, Gα, and Aβ resonances.

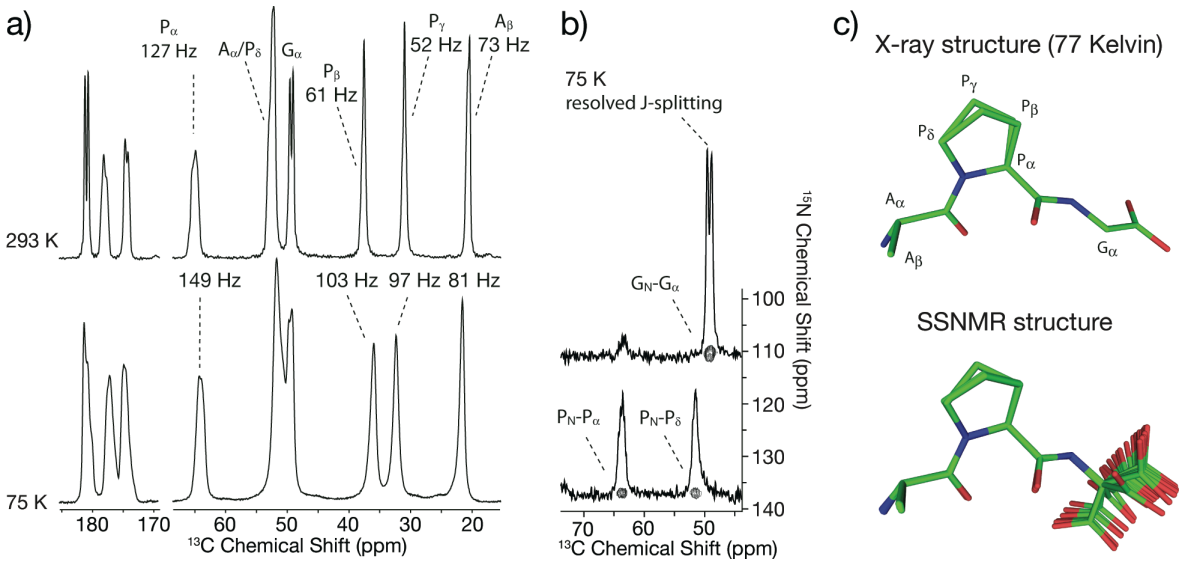

Fig. 3 High-resolution spectra of APG showing low temperature heterogeneous broadening only for the 3 carbon resonances that sample two puckered conformations. a) ^{13}C spectra of APG at 293 and 75 K. b) The carbon aliphatic region of a ^{15}N-^{13}C correlation spectrum with 1D direct ^{13}C dimension slices overlaid on the 2D contours. c) X-Ray and solid state NMR structures of APG from Barnes *et al*.[25]

In fact, a ^{13}C-^{13}C J-coupling is resolved at Gα in the ^{15}N-^{13}C correlation spectrum (Fig. 3b). The three sites that do show broadening are on the proline ring; the Pβ and Pγ resonances (Fig. 3a) and the Pδ resonance (Fig. 3b) broaden by ~40 Hz. We attribute this to conformational heterogeneity in the five-membered ring (Fig. 3c) which is currently under investigation.

Efficient and uniform polarization distribution via proton spin diffusion

The ^{15}N 1D DNP CPMAS spectrum of light-adapted [U-^{13}C,^{15}N]-bR is shown in Fig. 4. The buried Schiff base at 165 ppm is well resolved from the amide, arginine and other lysine sidechain nitrogen resonances. To address whether the enhanced polarization originating from the electron spins and DNP is uniformly distributed across the membrane, and the protein embedded therein, we integrated the intensity of the four separated lineshapes in the ^{15}N spectrum in Fig. 4. If the polarization is uniformly distributed, the integral of each resonance should be proportional to the number of contributing nuclei. As shown in Table 1, the relative intensities of the resonances correspond very well to this expectation, providing clear evidence that the polarization propagates to the buried active site as thoroughly as to the rest of the protein embedded in its native membrane. Proton spin diffusion thus effectively transfers the DNP enhanced polarization throughout the heterogenous sample of cyroprotectant and membrane protein in lipid bilayers.

Accelerated Data Acquisition

In the original expression for the sensitivity enhancement from the classical CP experiment, the ratio of the spin-lattice relaxation times of the abundant and rare spins (T_{1S}/T_{1I}) plays an important role.[26] This term represents the gain in time savings from utilizing the shorter spin-lattice relaxation time of ^{1}H magnetization versus ^{13}C or ^{15}N. This is important as

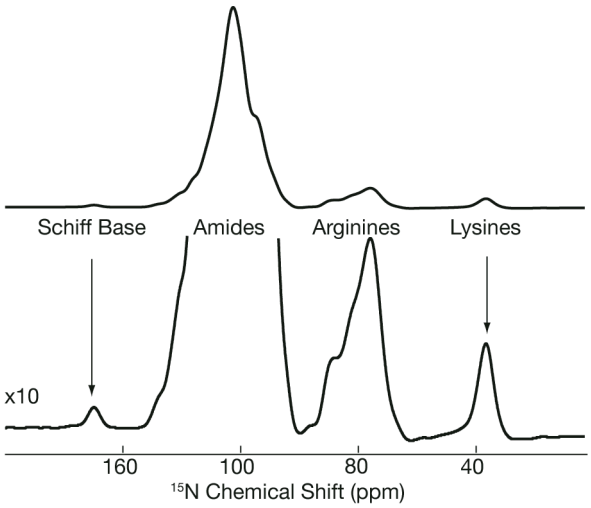

Fig. 4 1D ^{15}N spectrum of U-[^{13}C,^{15}N]-bR showing the ^{15}N Schiff base resonance adjacent to the peptide backbone signal.

Table 1 Relative experimental intensities (peak areas) of a DNP enhanced ^{15}N spectrum of bR *vs*. number of ^{15}N sites present.

Peak Assignment	Peak Area	Number of Sites
Schiff Base	1	1
Amides	240 ± 13	248
Arginines	25 ± 2	21
Lysines	6 ± 1	6

the experimental gain in sensitivity between a Bloch decay and CP experiment is typically only a factor of ~2.5 versus the theoretical maximum of 4.[27] Thus much of the improvement in sensitivity from using CP actually comes from the reduced time needed to recover longitudinal magnetization between signal averaging transients. The situation is similar in DNP experiments, although the polarization enhancements are of course much larger.

The radical concentration, initial electron to nuclear polarization transfer rate, and proton spin diffusion efficiency govern the rate of longitudinal build up of magnetization during the polarization period between DNP/MAS signal averaging transients. This time constant differs from classical NMR experiments in which the rate of recovery of longitudinal magnetization is dependent on the spectral density function evaluated at the nuclear Larmor frequency. Optimal repetition rates of DNP/MAS experiments at cryogenic temperatures are thus much higher than for samples without paramagnetic dopants. This has recently been exploited at ambient temperatures to reduce the proton T_1, which leads to much improved repetition rates and sensitivity.[28] Here we show that similar improvements in data acquisition rates are seen by increasing the concentration of polarizing agents in DNP experiments.

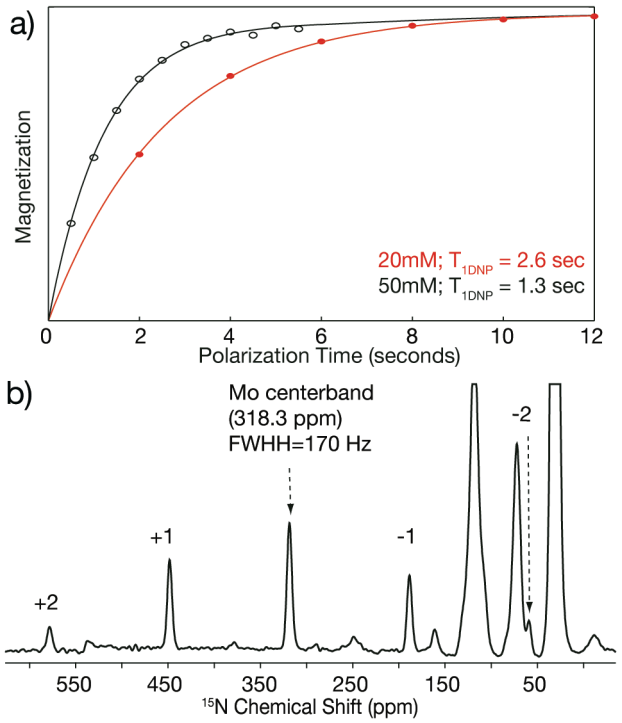

Fig. 5 Accelerated DNP. a) difference in longitudinal relaxation time, T_{1DNP}, under microwave irradiation between 20 and 50 mM TOTAPOL. The magnetization of the bulk protons is measured via CP to the carbonyls of [U-^{15}N,^{13}C]-bR. b) DNP spectrum of [ζ-^{15}N]lysine-labeled bR trapped in the M_o photocycle intermediate. 81,920 Transients, 1.6 s recycle delay, 36.4 hr acquisition time, $\omega_r/2\pi$ = 5000 Hz, T=89 K. The isotropic shift is 318.3 ppm, the span is 620 ppm, the skew is –0.034, and the tensor elements are: δ_{11} = 618, δ_{22}=340, and δ_{33}=–2.5 ppm.

As shown in Fig. 5a, increasing the biradical concentration from 20 mM to 50 mM reduces the longitudinal proton magnetization build-up time constant (T_{1DNP}) by a factor of two, thus doubling the rate of signal averaging. Relatively short recycle delays of 1.6 s (1.26*T_{1DNP}) for experiments on [ζ–^{15}N]lysine labeled bR were used to exploit the short proton T_1. Due to the cryogenic temperatures, extensive cooling power from the spinning gases, and the use of thermally conductive sapphire rotors, the sample is not at risk of detrimental heating that can arise from high RF power and short delays between transients at ambient temperatures.

Fig. 5b shows spectra of the M_o photocycle intermediate after only 1.5 days of signal averaging. There is sufficient signal-to-noise to complete a Herzfeld-Berger analysis[29] and extract the chemical shift anisotropy parameters, which are given in the figure caption. Even the +2 sideband with only a small fraction of the intensity of the centerband, corresponding to an effective sensitivity expected from a 700 kDa protein, has sufficient signal-to-noise to be fitted and used in the chemical shift analysis.

The resolution in the ^{15}N resonance in the active site is not broadened even when the electron concentration is increased to 100 mM. The linewidth of the Schiff base resonance is the same at 50 mM TOTAPOL as at when 15 mM.. The biradical is excluded from the center of the protein by steric hindrance and paramagnetic electrons are not close enough to the active site to result in pseudo-contact shifts and broadening.

Conclusions

Excellent resolution and sensitivity are available in cryogenic MAS DNP spectra of membrane proteins and crystalline peptides. With proper cyroprotection, similar linewidths to those reported here should be achievable on crystalline proteins and other integral membrane proteins.

Acknowledgements

This research was supported by the National Institutes of Health through grants EB002804, EB003151 and EB002026 to RGG, EB001035 to JH, and EB001965 and EB004866 to RJT. ABB and LBA were partially supported by graduate research fellowships from the National Science Foundation. Stimulating conversations with T. Maly and M. Bayro are gratefully acknowledged.

References

1. T. R. Carver and C. P. Slichter, *Phys. Rev.*, 1956, **102**, 975-980.
2. A. Abragam and M. Goldman, *Reports on Progress in Physics*, 1978, 395.
3. A. Barnes, G. De Paëpe, P. van der Wel, K. Hu, C. Joo, V. Bajaj, M. Mak-Jurkauskas, J. Sirigiri, J. Herzfeld and R. Temkin, *Appl. Magn. Reson.*, 2008, **34**, 237-263.
4. M. L. Mak-Jurkauskas, V. S. Bajaj, M. K. Hornstein, M. Belenky, R. J. Temkin, R. G. Griffin and J. Herzfeld, *Proc. Natl. Acad. Sci. U. S. A.*, 2008, **105**, 883-888.

5. M. Rosay, J. C. Lansing, K. C. Haddad, W. W. Bachovchin, J. Herzfeld, R. J. Temkin and R. G. Griffin, *J. Am. Chem. Soc.*, 2003, **125**, 13626-13627.
6. G. T. Debelouchina, M. J. Bayro, P. C. A. van der Wel, M. Caproini, A. B. Barnes, M. Rosay, M. Werner and R. G. Griffin, *Physical Chemistry and Chemical Physics*, 2010, **XX**, XX-XXX.
7. P. C. A. van der Wel, K.-N. Hu, J. R. Lewandowski and R. G. Griffin, *Journal of the American Chemical Society*, 2006, **128**, 10840-10846.
8. C. Song, K.-N. Hu, T. M. Swager and R. G. Griffin, *J. Am Chem. Soc*, 2006, **128**, 11385-11390.
9. K.-N. Hu, C. Song, H.-h. Yu, T. M. Swager and R. G. Griffin, *Jounal of Chemical Physics*, 2008, **128**, 052302.
10. L. R. Becerra, G. J. Gerfen, R. J. Temkin, D. J. Singel and R. G. Griffin, *Phys. Rev. Lett.*, 1993, **71**, 3561-3564.
11. P. S. Nadaud, J. J. Helmus, N. H√∂fer and C. P. Jaroniec, *Journal of the American Chemical Society*, 2007, **129**, 7502-7503.
12. J. M. Griffiths, K. V. Lakshmi, A. E. Bennett, J. Raap, C. M. Vanderwielen, J. Lugtenburg, J. Herzfeld and R. G. Griffin, *Journal of the American Chemical Society*, 1994, **116**, 10178-10181.
13. K.-N. Hu, H.-h. Yu, T. M. Swager and R. G. Griffin, *Journal of the American Chemical Society*, 2004, **126**, 10844-10845.
14. D. Oesterhelt and W. Stoeckenius, *Proceedings of the National Academy of Sciences*, 1973, **70**, 2853.
15. P. Argade, K. Rothschild, A. Kawamoto, J. Herzfeld and W. Herlihy, *Proceedings of the National Academy of Sciences*, 1981, **78**, 1643.
16. A. B. Barnes, M. L. Mak-Jurkauskas, Y. Matsuki, V. S. Bajaj, P. C. A. van der Wel, R. DeRocher, J. Bryant, J. R. Sirigiri, R. J. Temkin, J. Lugtenburg, J. Herzfeld and R. G. Griffin, *Journal of Magnetic Resonance*, 2009, **198**, 261-270.
17. K. E. Kreischer, C. Farrar, R. G. Griffin, R. J. Temkin and J. Vieregg, in *Proceedings of the 24th International Conference on Infrared and Millimeter Waves*, ed. L. Lombardo, UC Davis, Monterey, CA, 1999, pp. TU-A3.
18. V. S. Bajaj, M. K. Hornstein, K. E. Kreischer, J. R. Sirigiri, P. P. Woskov, M. Mak, J. Herzfeld, R. J. Temkin and R. G. Griffin, *Journal of Magnetic Resonance*, 2007, **190**, 86-114.
19. P. W. Woskov, V. S. Bajaj, M. K. Hornstein, R. J. Temkin and R. G. Griffin, *IEEE Transactions on Microwave Theory and Techniques*, 2005, **53**, 1863-1869.
20. P. J. Allen, F. Creuzet, H. J. M. de Groot and R. G. Griffin, *Journal of Magnetic Resonance*, 1991, **92**, 614-617.
21. V. Bajaj, M. Mak-Jurkauskas, M. Belenky, J. Herzfeld and R. Griffin, *Proceedings of the National Academy of Sciences*, 2009, **106**, 9244.
22. V. S. Bajaj, P. C. A. van der Wel and R. G. Griffin, *Journal of the American Chemical Society*, 2009, **131**, 118-128.
23. R. Poupko, Z. Luz and H. Zimmermann, *Journal of the American Chemical Society*, 1982, **104**, 5307-5314.
24. E. Wells, R. Ferguson, J. Hallett and L. Peterson, *Canadian Journal of Chemistry*, 1968, **46**, 2733-2742.
25. A. B. Barnes, L. B. Andreas, M. Huber, R. Ramachandran, P. C. A. van der Wel, M. Veshtort, R. G. Griffin and M. A. Mehta, *Journal of Magnetic Resonance*, 2009, **200**, 95-100.
26. A. Pines, M. G. Gibby and J. S. Waugh, *J. Chem. Phys.*, 1973, **59**, 569-590.
27. M. J. Bayro, N. R. Birkett, C. M. Dobson and R. G. Griffin, *Chemphyschem*, 2010, **submitted**.
28. N. Wickramasinghe, S. Parthasarathy, C. Jones, C. Bhardwaj, F. Long, M. Kotecha, S. Mehboob, L. Fung, J. Past and A. Samoson, *Nature methods*, 2009, **6**, 215.
29. J. Herzfeld and A. E. Berger, *Journal of Chemical Physics*, 1980, **73**, 6021-6030.